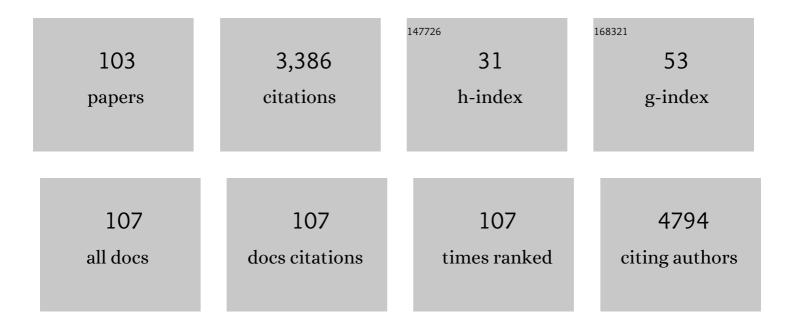
List of Publications by Year in descending order

Source: https://exaly.com/author-pdf/2023367/publications.pdf Version: 2024-02-01



ΗΙςλομι Τλνιλκλ

#	Article	IF	CITATIONS
1	Effect of urinary glucose concentration and pH on signal intensity in magnetic resonance images. Japanese Journal of Radiology, 2022, , 1.	1.0	Ο
2	The applications of plasma cell-free DNA in cancer detection: Implications in the management of breast cancer patients. Critical Reviews in Oncology/Hematology, 2022, 175, 103725.	2.0	1
3	The fragility of a structurally diverse duplication block triggers recurrent genomic amplification. Nucleic Acids Research, 2021, 49, 244-256.	6.5	7
4	Quantitative assessment reveals the dominance of duplicated sequences in germline-derived extrachromosomal circular DNA. Proceedings of the National Academy of Sciences of the United States of America, 2021, 118, .	3.3	18
5	Mutant POLQ and POLZ/REV3L DNA polymerases may contribute to the favorable survival of patients with tumors with POLE mutations outside the exonuclease domain. BMC Medical Genetics, 2020, 21, 167.	2.1	2
6	Mechanisms Underlying Recurrent Genomic Amplification in Human Cancers. Trends in Cancer, 2020, 6, 462-477.	3.8	43
7	Tumors defective in homologous recombination rely on oxidative metabolism: relevance to treatments with <scp>PARP</scp> inhibitors. EMBO Molecular Medicine, 2020, 12, e11217.	3.3	37
8	Differentiating between Glioblastoma and Primary CNS Lymphoma Using Combined Whole-tumor Histogram Analysis of the Normalized Cerebral Blood Volume and the Apparent Diffusion Coefficient. Magnetic Resonance in Medical Sciences, 2019, 18, 53-61.	1.1	14
9	Towards prognostic functional brain biomarkers for cervical myelopathy: A resting-state fMRI study. Scientific Reports, 2019, 9, 10456.	1.6	26
10	Quantifying the Severity of Parkinson Disease by Use of Dopaminergic Neuroimaging. American Journal of Roentgenology, 2019, 213, 163-168.	1.0	8
11	Quantitative evaluation of blood flow in each cerebral branch associated with zone 1–2 thoracic endovascular aortic repair. European Journal of Cardio-thoracic Surgery, 2019, 55, 1079-1085.	0.6	3
12	Quantifying changes in nigrosomes using quantitative susceptibility mapping and neuromelanin imaging for the diagnosis of early-stage Parkinson's disease. British Journal of Radiology, 2018, 91, 20180037.	1.0	41
13	Comparative study of pulsed-continuous arterial spin labeling and dynamic susceptibility contrast imaging by histogram analysis in evaluation of glial tumors. Neuroradiology, 2018, 60, 599-608.	1.1	14
14	FOXC1-induced non-canonical WNT5A-MMP7 signaling regulates invasiveness in triple-negative breast cancer. Oncogene, 2018, 37, 1399-1408.	2.6	67
15	circRNA meets gene amplification. Non-coding RNA Investigation, 2018, 2, 38-38.	0.6	2
16	BRCA1 ensures genome integrity by eliminating estrogen-induced pathological topoisomerase II–DNA complexes. Proceedings of the National Academy of Sciences of the United States of America, 2018, 115, E10642-E10651.	3.3	75
17	Emerin Deregulation Links Nuclear Shape Instability to Metastatic Potential. Cancer Research, 2018, 78, 6086-6097.	0.4	49
18	Quantitative Comparison of Virtual Monochromatic Images of Dual Energy Computed Tomography Systems. Journal of Computer Assisted Tomography, 2018, 42, 648-654.	0.5	11

#	Article	IF	CITATIONS
19	Complex repeat structure promotes hyper-amplification and amplicon evolution through rolling-circle replication. Nucleic Acids Research, 2018, 46, 5097-5108.	6.5	2
20	Large extracellular vesicles carry most of the tumour DNA circulating in prostate cancer patient plasma. Journal of Extracellular Vesicles, 2018, 7, 1505403.	5.5	286
21	Multiple blood flow measurements before and after carotid artery stenting via phase-contrast magnetic resonance imaging: An observational study. PLoS ONE, 2018, 13, e0195099.	1.1	4
22	Palindromic amplification of the ERBB2 oncogene in primary HER2-positive breast tumors. Scientific Reports, 2017, 7, 41921.	1.6	28
23	Vessel-Masked Perfusion Magnetic Resonance Imaging With Histogram Analysis Improves Diagnostic Accuracy for the Grading of Glioma. Journal of Computer Assisted Tomography, 2017, 41, 910-915.	0.5	5
24	Whole-tumor histogram analysis of the cerebral blood volume map: tumor volume defined by 11C-methionine positron emission tomography image improves the diagnostic accuracy of cerebral glioma grading. Japanese Journal of Radiology, 2017, 35, 613-621.	1.0	4
25	Impediment of Replication Forks by Long Non-coding RNA Provokes Chromosomal Rearrangements by Error-Prone Restart. Cell Reports, 2017, 21, 2223-2235.	2.9	13
26	Comparison of Silent and Conventional MR Imaging for the Evaluation of Myelination in Children. Magnetic Resonance in Medical Sciences, 2017, 16, 209-216.	1.1	18
27	Heritability of brain volume on MRI in middle to advanced age: A twin study of Japanese adults. PLoS ONE, 2017, 12, e0175800.	1.1	12
28	Impact of neoadjuvant HER2-directed therapy on HER2 status in breast cancer Journal of Clinical Oncology, 2017, 35, e12130-e12130.	0.8	0
29	Reduction of misregistration on cerebral four-dimensional computed tomography angiography images using advanced patient motion correction reconstruction. Japanese Journal of Radiology, 2016, 34, 605-610.	1.0	2
30	Comparison of diffusion tensor imaging and 11C-methionine positron emission tomography for reliable prediction of tumor cell density in gliomas. Journal of Neurosurgery, 2016, 125, 1136-1142.	0.9	16
31	Right cerebellar infarction due to ipsilateral neck-rotation-induced right vertebral artery compression and occlusion, demonstrated by CT angiography. Radiology Case Reports, 2015, 10, 1025.	0.2	1
32	Replication fork integrity and intra-S phase checkpoint suppress gene amplification. Nucleic Acids Research, 2015, 43, 2678-2690.	6.5	19
33	Adult hemimegalencephaly associated with multiple cerebral aneurysms. Neurology, 2015, 84, 2460-2461.	1.5	1
34	Model-based iterative reconstruction for detection of subtle hypoattenuation in early cerebral infarction: a phantom study. Japanese Journal of Radiology, 2015, 33, 26-32.	1.0	25
35	FOXC1 Activates Smoothened-Independent Hedgehog Signaling in Basal-like Breast Cancer. Cell Reports, 2015, 13, 1046-1058.	2.9	124
36	Neuromelanin Magnetic Resonance Imaging Reveals Increased Dopaminergic Neuron Activity in the Substantia Nigra of Patients with Schizophrenia. PLoS ONE, 2014, 9, e104619.	1.1	48

#	Article	IF	CITATIONS
37	Dual-energy CT for detection of contrast enhancement or leakage within high-density haematomas in patients with intracranial haemorrhage. Neuroradiology, 2014, 56, 291-295.	1.1	23
38	Prevalence and diagnostic performance of computed tomography angiography spot sign for intracerebral hematoma expansion depend on scan timing. Neuroradiology, 2014, 56, 1039-1045.	1.1	22
39	CAP-Seq: a method for identification of DNA palindromes. BMC Genomics, 2014, 15, 394.	1.2	10
40	Three-dimensional topographical variation of femoral cartilage T2 in healthy volunteer knees. Skeletal Radiology, 2013, 42, 363-370.	1.2	24
41	Changes in endolymphatic hydrops after sac surgery examined by Gd-enhanced MRI. Acta Oto-Laryngologica, 2013, 133, 924-929.	0.3	37
42	Homology-mediated end-capping as a primary step of sister chromatid fusion in the breakage-fusion-bridge cycles. Nucleic Acids Research, 2013, 41, 9732-9740.	6.5	17
43	Whole-body MR Imaging in Detecting Phosphaturic Mesenchymal Tumor (PMT) in Tumor-induced Hypophosphatemic Osteomalacia. Magnetic Resonance in Medical Sciences, 2013, 12, 47-52.	1.1	17
44	Assessment of palindromes as platforms for DNA amplification in breast cancer. Genome Research, 2012, 22, 232-245.	2.4	31
45	Accurate bone registration in knee MR images. Journal of the Chinese Institute of Engineers, Transactions of the Chinese Institute of Engineers,Series A/Chung-kuo Kung Ch'eng Hsuch K'an, 2012, 35, 101-113.	0.6	1
46	Cardiac Cycle-Related Volume Change in Unruptured Cerebral Aneurysms. Stroke, 2012, 43, 61-66.	1.0	26
47	A common copy-number breakpoint of ERBB2 amplification in breast cancer colocalizes with a complex block of segmental duplications. Breast Cancer Research, 2012, 14, R150.	2.2	26
48	Usefulness of contrast-enhanced three-dimensional MR angiography using time-resolved imaging of contrast kinetics applied to description of Extracranial Arteriovenous Malformations: Initial Experience. European Journal of Radiology, 2012, 81, 1134-1139.	1.2	15
49	Molecular Trajectories Leading to the Alternative Fates of Duplicate Genes. PLoS ONE, 2012, 7, e38958.	1.1	8
50	Automatic 3D MR Image Registration and Its Evaluation for Precise Monitoring of Knee Joint Disease. IEICE Transactions on Information and Systems, 2011, E94-D, 698-706.	0.4	0
51	Capillary Hemangioma in a Rib Presenting as Large Pleural Effusion. Annals of Thoracic Surgery, 2011, 91, e59-e61.	0.7	11
52	Variation in supratentorial cerebrospinal fluid production rate in one day: measurement by nontriggered phase-contrast magnetic resonance imaging. Japanese Journal of Radiology, 2011, 29, 110-115.	1.0	10
53	Genome-wide analysis of palindrome formation. Nature Genetics, 2010, 42, 279-279.	9.4	5
54	DNA methylation of developmental genes in pediatric medulloblastomas identified by denaturation analysis of methylation differences. Proceedings of the National Academy of Sciences of the United States of America, 2010, 107, 234-239.	3.3	59

#	Article	IF	CITATIONS
55	Loaded Cartilage T2 Mapping in Patients with Hip Dysplasia. Radiology, 2010, 256, 955-965.	3.6	46
56	Linkage Disequilibrium between Two High-Frequency Deletion Polymorphisms: Implications for Association Studies Involving the glutathione-S transferase (GST) Genes. PLoS Genetics, 2009, 5, e1000472.	1.5	44
57	Effect of flip angle on volume flow measurement with nontriggered phaseâ€contrast MR: In vivo evaluation in carotid and basilar arteries. Journal of Magnetic Resonance Imaging, 2009, 29, 1218-1223.	1.9	3
58	Palindromic gene amplification — an evolutionarily conserved role for DNA inverted repeats in the genome. Nature Reviews Cancer, 2009, 9, 216-224.	12.8	86
59	Use of fractional anisotropy for determination of the cut-off value in 11C-methionine positron emission tomography for glioma. Neurolmage, 2009, 45, 312-318.	2.1	27
60	Phase-contrast MR Studies of CSF Flow Rate in the Cerebral Aqueduct and Cervical Subarachnoid Space with Correlation-based Segmentation. Magnetic Resonance in Medical Sciences, 2009, 8, 91-100.	1.1	30
61	A Hybrid Technique for Thickness-Map Visualization of the Hip Cartilages in MRI. IEICE Transactions on Information and Systems, 2009, E92-D, 2253-2263.	0.4	3
62	Fractional anisotropy and tumor cell density of the tumor core show positive correlation in diffusion tensor magnetic resonance imaging of malignant brain tumors. Neurolmage, 2008, 43, 29-35.	2.1	149
63	Intrastrand Annealing Leads to the Formation of a Large DNA Palindrome and Determines the Boundaries of Genomic Amplification in Human Cancer. Molecular and Cellular Biology, 2007, 27, 1993-2002.	1.1	57
64	A Fully Automated Method for Segmentation and Thickness Map Estimation of Femoral and Acetabular Cartilages in 3D CT Images of the Hip. Proc Int Symp Image Signal Process Anal, 2007, , .	0.0	4
65	MRI and CT findings of the giant cell tumors of the skull; five cases and a review of the literature. European Journal of Radiology, 2006, 58, 435-443.	1.2	32
66	Large DNA palindromes as a common form of structural chromosome aberrations in human cancers. Human Cell, 2006, 19, 17-23.	1.2	29
67	Quantitative study of changes in oxidative metabolism during visual stimulation using absolute relaxation rates. NMR in Biomedicine, 2006, 19, 60-68.	1.6	21
68	Assessment of the three-dimensional relationship of the ossific nuclei and cartilaginous anlagen in congenital clubfoot by 3-D MRI. Journal of Orthopaedic Research, 2005, 23, 1160-1164.	1.2	29
69	Widespread and nonrandom distribution of DNA palindromes in cancer cells provides a structural platform for subsequent gene amplification. Nature Genetics, 2005, 37, 320-327.	9.4	95
70	Fat-Suppressed 3D Spoiled Gradient-Echo MRI and MDCT Arthrography of Articular Cartilage in Patients with Hip Dysplasia. American Journal of Roentgenology, 2005, 185, 379-385.	1.0	79
71	Determination of transverse relaxation rate for estimating iron deposits in central nervous system. Neuroscience Research, 2005, 51, 67-71.	1.0	33
72	Abstract of Symposium. Human Cell, 2005, 18, 29-33.	1.2	0

#	Article	IF	CITATIONS
73	Three-dimensional distribution of acetabular cartilage thickness in patients with hip dysplasia: a fully automated computational analysis of MR imaging. Osteoarthritis and Cartilage, 2004, 12, 650-657.	0.6	88
74	Clinical accuracy evaluation of femoral canal preparation using the ROBODOC system. Journal of Orthopaedic Science, 2004, 9, 452-461.	0.5	53
75	Origin of High Signal Intensity in the Cavernous Sinus in MR Angiographic Source Images. Journal of Computer Assisted Tomography, 2004, 28, 728-734.	0.5	7
76	Comparison of the fit and fill between the Anatomic Hip femoralcomponent and the VerSys Taper femoral component using virtualimplantation on the ORTHODOC workstation. Journal of Orthopaedic Science, 2003, 8, 352-360.	0.5	27
77	Quantitative mapping of cerebral deoxyhemoglobin content using MR imaging. NeuroImage, 2003, 20, 2071-2083.	2.1	33
78	Limits on the accuracy of 3-D thickness measurement in magnetic resonance images- Effects of voxel anisotropy. IEEE Transactions on Medical Imaging, 2003, 22, 1076-1088.	5.4	30
79	Short inverted repeats initiate gene amplification through the formation of a large DNA palindrome in mammalian cells. Proceedings of the National Academy of Sciences of the United States of America, 2002, 99, 8772-8777.	3.3	105
80	Low Incidence of p53 Mutations in Well-differentiated Tongue Squamous Cell Carcinoma in Japan. Japanese Journal of Clinical Oncology, 2002, 32, 327-331.	0.6	3
81	Effects of stimulus presentation rate on the activity of primary somatosensory cortex: a functional magnetic resonance imaging study in humans. Brain Research Bulletin, 2001, 54, 125-129.	1.4	4
82	A fully automated method for segmentation and thickness determination of hip joint cartilage from 3D MR data. International Congress Series, 2001, 1230, 352-358.	0.2	15
83	Articular Cartilage Abnormalities in Dysplastic Hips Without Joint Space Narrowing. Clinical Orthopaedics and Related Research, 2001, 383, 183-190.	0.7	42
84	Postradiation sarcomas of the pelvis after treatment for uterine cervical cancer: review of the CT and MR findings of five cases. Skeletal Radiology, 2001, 30, 132-137.	1.2	13
85	MR-based three-dimensional presentation of cartilage thickness in the femoral head. European Radiology, 2001, 11, 2178-2183.	2.3	30
86	Limits to the Accuracy of 3D Thickness Measurement in Magnetic Resonance Images. Lecture Notes in Computer Science, 2001, , 803-810.	1.0	5
87	Effects of stimulus rate on the auditory cortex using fMRI with â€~sparse' temporal sampling. NeuroReport, 2000, 11, 2045-2049.	0.6	32
88	Proton magnetic resonance spectroscopy of patients with parkinsonism. Brain Research Bulletin, 2000, 52, 589-595.	1.4	76
89	Solitary subependymal giant cell astrocytoma: case report. European Journal of Radiology, 2000, 33, 55-58.	1.2	29
90	Movement-Related Desynchronization of the Cerebral Cortex Studied with Spatially Filtered Magnetoencephalography. NeuroImage, 2000, 12, 298-306.	2.1	199

#	Article	IF	CITATIONS
91	Bone Metastases from Soft Tissue Sarcomas. Seminars in Musculoskeletal Radiology, 1999, 3, 183-189.	0.4	15
92	Characterization of six cell lines established from human pancreatic adenocarcinomas. , 1999, 85, 832-840.		29
93	Lymph node metastasis is associated with allelic loss on chromosome 13q12-13 in esophageal squamous cell carcinoma. Cancer Research, 1999, 59, 3724-9.	0.4	23
94	Juxta-articular ankylosis of the temporomandibular joint as an unusual cause of limitation of mouth opening: Case report. Journal of Oral and Maxillofacial Surgery, 1998, 56, 243-246.	0.5	13
95	Functional mapping of pain-related activation with echo-planar MRI. NeuroReport, 1998, 9, 2285-2289.	0.6	35
96	Transition of the Craniocaudal Velocity of the Spinal Cord. Investigative Radiology, 1998, 33, 141-145.	3.5	13
97	Methylation of the 5' CpG island of the FHIT gene is closely associated with transcriptional inactivation in esophageal squamous cell carcinomas. Cancer Research, 1998, 58, 3429-34.	0.4	110
98	Multiple types of aberrations in thep16 (INK4a) and thep15(INK4b) genes in 30 esophageal squamous-cell-carcinoma cell lines. , 1997, 70, 437-442.		42
99	Genetic Alterations in Patients With Esophageal Cancer With Short- and Long-Term Survival Rates After Curative Esophagectomy. Annals of Surgery, 1997, 226, 162-168.	2.1	49
100	Initial Experience with Helical CT and 3D Reconstruction in Therapeutic Planning of Cerebral AVMs: Comparison with 3D Time-of-Flight MRA and Digital Subtraction Angiography. Journal of Computer Assisted Tomography, 1997, 21, 811-817.	0.5	47
101	Simple bone cyst of the mandibular condyle: Report of a case. Journal of Oral and Maxillofacial Surgery, 1996, 54, 1454-1458.	0.5	23
102	Characterization ofp53 gene mutations in esophageal squamous cell carcinoma cell lines: Increased frequency and different spectrum of mutations from primary tumors. , 1996, 65, 372-376.		46
103	Intraosseous ganglion. Skeletal Radiology, 1995, 24, 155-7.	1.2	14